

## EMITTER AND CONTACT OPTIMIZATION FOR HIGH-EFFICIENCY IBC MERCURY CELLS

<sup>1</sup>Agnes Mewe, <sup>1</sup>Pierpaolo Spinelli, <sup>1</sup>Antonius Burgers, <sup>2</sup>Ard Vlooswijk, <sup>1</sup>Nicolas Guillevin, <sup>1</sup>Eric Kossen, <sup>1</sup>Ilkay Cesar

<sup>1</sup>ECN Solar Energy, Petten, NL-1755 LE, The Netherlands

Tel: +31 88 515 4323; Fax: +31 88 515 8214; E-mail: [mewe@ecn.nl](mailto:mewe@ecn.nl)

<sup>2</sup>Tempres Systems, Vaassen, NL-8171 MD, The Netherlands

**ABSTRACT:** In this paper we present the results of a study of the emitter contact properties of the Mercury cell, which is an n-type IBC cell with a front floating emitter. We found that contact recombination becomes higher and contact resistance becomes lower with higher firing temperature. Additionally, the contacts to light and heavy emitters were evaluated and the results showed that in case of a heavier emitter, the emitter contact recombination is reduced. The emitter contact resistance to both the light and heavy emitter appeared to only depend on the sheet resistance, but not on the exact shape of the doping profile. The contact recombination, calculated from measured  $V_{oc}$  values of test structures, appeared to be dependent on which side of the sample was illuminated: extracted  $V_{oc}$  values from front side illumination lead to much lower fitted  $J_{0,contact}$  values than from rear side illumination. Quokka simulations indicate that the lower front side illumination values are closer to the real values, which can be calculated from the results of the measurements with either orientation.

**Keywords:** Back Contact, c-Si, Characterisation, Contact, Metallization, n-type, Recombination, Screen Printing

### 1 LOSSES IN MERCURY IBC CELLS

The Mercury cell which we developed at ECN is an interdigitated back contact (IBC) cell which features a front floating emitter (FFE). This FFE enhances lateral transport of holes and limits the effect of electrical shading [1], enabling easy module integration. In Figure 1, a schematic cross-section of the Mercury cell is shown.

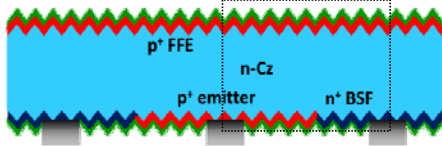


**Figure 1:** Schematic cross-section of the Mercury cell, with the unit cell, as used in simulations, indicated

Recently, we published improvement of our best Mercury cell to 21.1% [2], still following an industrial process flow that uses the same equipment as we use for our industrial n-Pasha cell.

#### 1.1 Loss analysis

We performed a loss analysis of the Mercury cell. The bulk and surface recombination and transport losses are based on 2D device physics with Quokka [3] on a cross-section of the unit cell. The ohmic losses related to metal patterns are based on the calculated contact and line resistance of the fingers and busbars. Finally, circuit simulations were used to include several edge (non-unit-cell) effects.

The loss analysis that we performed on these cells, revealed that we suffer from important losses in our emitter contact, both recombination as well as ohmic losses. The loss analysis breakdown is shown in Figure 2.

#### 1.2 Emitter contact

The loss breakdown shows us that, besides the emitter contact, the other large contributor to the losses is the n-Cz bulk. The bulk shows high ohmic losses as high-ohmic material was considered, and these could be partly mitigated when thinner and/or medium resistivity wafers

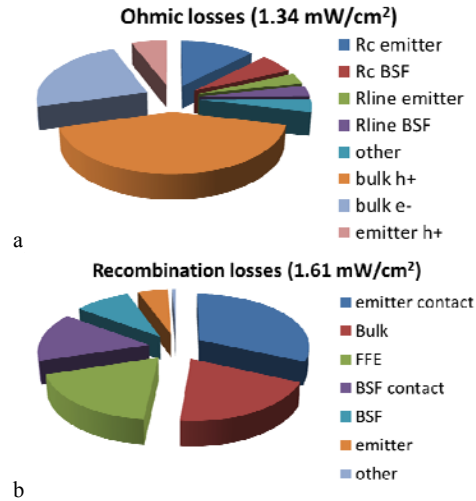


**Figure 2:** Loss analysis breakdown of the Mercury IBC cell, split in a) ohmic and b) recombination losses

are used. Considering the metal contact losses, the emitter contact recombination has the largest contribution and needs to be reduced. The losses in the BSF contacts are much smaller. The recombination in the FFE is considerable and can be further reduced by application of a lighter boron doping of 150  $\Omega$ /sq, which will be presented in this paper as well.

Based on these findings, we investigated the effects of different pastes and contact firing on the contact properties (contact resistance and contact recombination). Additionally, we made emitters with different  $R_{sheet}$  and doping profiles by varying the thermal diffusion process and by different etch-back of the as-diffused emitters.

In this paper we present the results of both routes to improve the emitter contact.

## 2 MEASUREMENT METHODS

### 2.1 Test structures

To evaluate the losses on a device which is processed

like an IBC cell, a special test structure was designed. Several key parameters can be evaluated, like contact recombination, as proposed in [4], and contact resistance, which we do from the combination of different structures on one wafer. This wafer is processed like an IBC cell, and differs only in the design of the doped areas and contacts.

### 2.2 $J_0$ fit from $V_{oc}$ measurement

Structures as depicted in Figure 3 can be used to fit the contact recombination parameter  $J_{0,c}$  by varying the contact area and evaluating the fitted  $J_{0l}$  (from a Suns- $V_{oc}$  measurement) as a function of metal contact area.

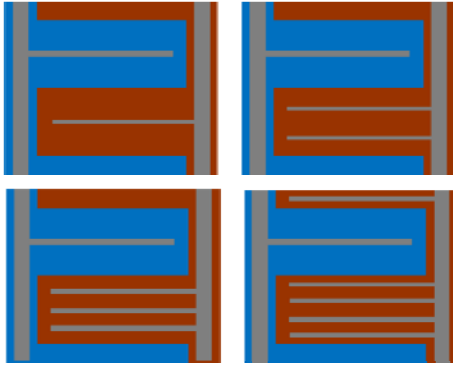


**Figure 3:** Test structures for measuring the emitter contact recombination. Blue and red indicate the BSF and emitter diffusions, grey the metallization

### 2.3 $R_{contact}$ using Transfer Length Method (TLM)

The transfer length method is used to determine the contact resistance of the emitter contact to the emitter. At ECN we use an automated TLM tool (PV-tools) that enables us to map the contact resistance over a complete wafer and to improve statistics, as the measurement is fast enough to evaluate several wafers per case.

## 3 INFLUENCE OF PASTE AND FIRING

We investigated the effect of the metal paste and the firing temperature on the contact properties. The contact recombination depends on how well the metal contact is shielded by the emitter, which depends on the doping profile (i.e. doping concentration as a function of depth) in combination with the etch depth of the metal paste into the doped layer (as schematically shown in Figure 4). The latter is related to paste chemistry and contact firing temperature, which are the parameters in this experiment. The same parameters will also influence the contact resistance.

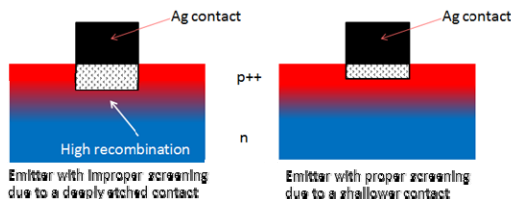


**Figure 4:** Schematic view of contact formation by a deep or shallow contact etch into the emitter profil

### 3.1 Set-up of experiment

Two different Ag/Al metal pastes were applied to a boron emitter with an industrial profile and a sheet resistance of  $70 \Omega/\text{sq}$ , and fired through the passivation layer using different firing temperatures. The set temperature differences in the firing furnace varied 40 to 60 °C for the two pastes, divided over 4 or 5 settings. Paste 1 is a commercially available Ag/Al paste, and paste 2 is a paste that was designed for improved contact properties, for which results on our n-Pasha concept were presented earlier this year [5].

The result of paste 3, also a commercially available paste, was added at one firing temperature setting to relate it to the emitter variation results in section 4.

### 3.2 Results

As shown in Figure 5, the  $J_{0,c}$  clearly increases with higher firing temperature. For the lowest temperatures, the  $J_{0,c}$  of the emitter contact can decrease down to below  $1500 \text{ fA}/\text{cm}^2$ , which is much lower compared to the  $J_0$  for a more standard firing setting ( $2000\text{-}2500 \text{ fA}/\text{cm}^2$ ).

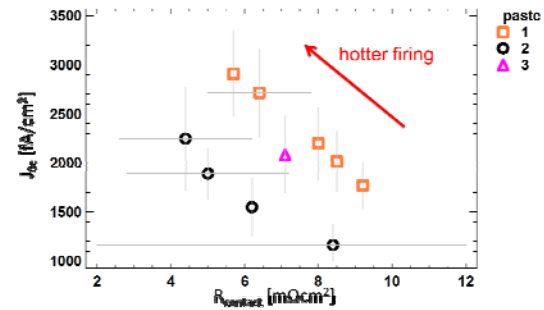


**Figure 5:** Fitted emitter contact recombination (vertical) against contact resistance (horizontal) for three different pastes for different firing settings (values towards higher firing temperature indicated)

The contact resistance of the fired metal contact to the emitter shows an opposite trend: it becomes higher for the lower temperatures. This means that in a cell, a balance should be found between contact resistance and recombination, to get the lowest cumulative losses and the highest performance. This will depend on the metallization geometry as well.

Paste 2 clearly performs better than paste 1 (and paste 3), which means that the combined ohmic and recombination losses in the cell will be smaller at the optimal firing setting.

### 3.3 Cells

The improved paste was used to make Mercury IBC cells, applying a slightly lighter doped emitter than tested in the contact properties experiment, as this is more optimal for the complete solar cell.

We applied the paste by screen printing and by stencil printing. Using stencil printing, we can achieve narrower fingers with better aspect ratio, which led to 2 mV higher  $V_{oc}$  due to the reduced emitter contact area, resulting in 0.1% absolute higher efficiency than the cells with screen printed metallization. The efficiency results are shown in Figure 6.

The average efficiency of the cells with stencil printed metallization was 21.0%, with the best cells reaching 21.1% (internal measurement, corrected for spectral mismatch), which equals our best cell result.

This is especially a promising result, because there are some processing factors that we already improved for the previously achieved best result and have not been included in this cell run. It means that there is definitely room for further improvement.

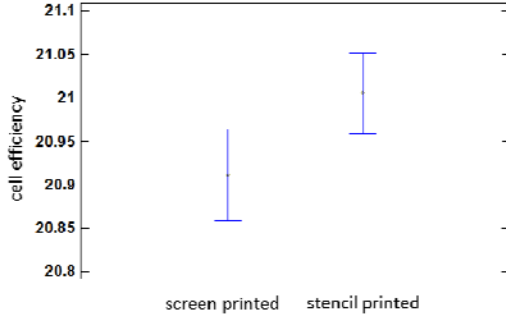


**Figure 6:** Efficiency results for Mercury cells with the improved emitter metallization paste (paste 2) using screen and stencil printing. Group sizes are 11 and 14 cells respectively

#### 4 INFLUENCE OF EMITTER PROFILE

In this experiment we investigated the effect of the doping profiles on contact recombination and contact resistance. As already mentioned, a deeper profile is associated with better contact shielding and therefore low contact recombination, as sketched in Figure 7.

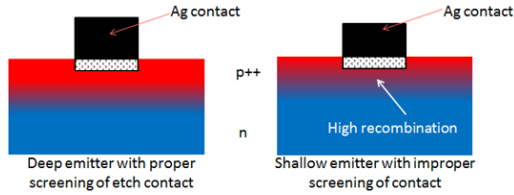


**Figure 7:** Schematic view of contact formation into a deep (heavy) or shallow doping profile

##### 4.1 Set-up of experiment

The different profiles were realized by changing the diffusion parameters (a standard light emitter and a heavy emitter) and additionally etching back to increase the sheet resistance to 50 (only for the heavy emitter), 70 and 85  $\Omega/\text{sq}$ . We used the previously mentioned paste 3 for the emitter contacts, and a standard firing setting.

##### 4.2 Results

In Figure 8 it is shown that the heavier emitter results in lower emitter contact recombination compared to the light emitter. Counterintuitively, etching back the same emitter profile does not lead to higher recombination values. For both emitter profiles, a clear trend of contact recombination with sheet resistance is absent.

As expected, for the contact resistance we observe a trend of higher  $R_{\text{contact}}$  with higher emitter  $R_{\text{sheet}}$ . Although the margin of error is quite large, the trend seems to be linear (not visible in the graph). There are no contact resistance differences between the heavy and light profiles with the same  $R_{\text{sheet}}$ .

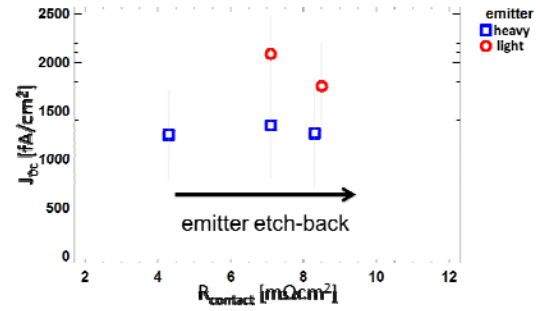


**Figure 8:** Fitted emitter contact recombination against contact resistance for a heavy emitter (blue) and more lightly doped emitter (red) after different etch-back (direction towards higher sheet resistance indicated)

##### 4.3 Outlook for cells

We conclude that we can further improve the cell results if we combine paste 2 with the contact properties of the heavy emitter.

Additionally, to avoid excessive recombination in the FFE, we can apply an etch-back on the front side, which is a good way to reduce losses in the cell further. The front floating emitter needs to remain conductive to allow lateral electron transport in an efficient way. From device simulations, we calculated that a FFE up to 150  $\Omega/\text{sq}$  is conductive enough and does not lead to additional ohmic losses.

In a test experiment on symmetrically diffused samples, we reduced the doping of the front floating emitter, to obtain sheet resistance values ranging from 70 to 150  $\Omega/\text{sq}$ , and evaluated the surface passivation on symmetric n-Cz samples with the boron FFE on each side. In Figure 9 the results of the  $J_0$  for one side are presented for five sample groups, which shows a 40% reduction of passivated surface  $J_0$  if we decrease the emitter  $R_{\text{sheet}}$  from 70 to almost 150  $\Omega/\text{sq}$ .

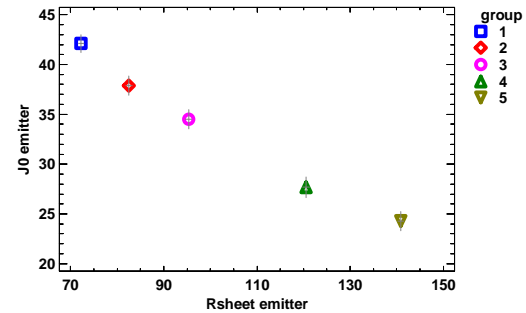


**Figure 9:** Emitter recombination decrease (single side evaluation of  $J_0$ , in  $\text{fA}/\text{cm}^2$ , with increasing FFE sheet resistance, in  $\Omega/\text{sq}$ )

The combined effects of paste and emitter choice, and a lighter FFE could result in 0.3-0.4% absolute efficiency gain, according to our simulations. This would bring our current record Mercury IBC cell of 21.1% (in-house measurement, corrected for spectral mismatch) to about 21.5% with only minor process changes.

## 5 DISCUSSION

### 5.1 Measurement method for $J_{0,c}$ fit

We fit the metal contact recombination parameter ( $J_{0,c}$ ) from the slope of the  $J_0$  with the metal fraction. The  $J_0$  is calculated from the  $V_{oc}$  that we measure. We executed the  $V_{oc}$  measurements of the test structures in this paper with the metallized side of the wafer facing the flash of the Suns- $V_{oc}$  set-up. This was done because of practical reasons, as we had to contact different locations of the test structures on the wafer, and therefore we need to put the contact probes on many different locations.

However, this procedure is not completely representative for the IBC cell, as the illuminated side of the test structure (metallized side) is different from the illuminated side of an IBC cell (non-metallized side). In addition to that, the varying metal coverage of the test structures may lead to errors in the measurements due to different light exposure of the cell.

To avoid this, we designed a printed circuit board that exactly matches with the contact locations of the test structures, so we can use it as a contacting chuck. All test structures can be individually contacted by correct placement and the measurement can be done with the non-metallized side up.

We compared the values that we obtained for the fitted contact recombination parameter using both orientations of the wafer (rear side up and front side up). In this case, the data came from samples with a lightly doped emitter from a different experiment. We found that the  $J_{0,c}$  values were quite different for the two orientations, as shown in Table I.

**Table I:** Fit of  $J_{0,c}$  values from  $V_{oc}$  measurements obtained with different sample orientations

Orientation	$J_{0,c}$ emitter [ $\text{fA}/\text{cm}^2$ ]
Front illumination	1217
Rear illumination	1834

We looked into this issue in more detail using Quokka simulations.

### 5.2 Quokka simulation results

We simulated the influence of the test structure orientation in the simulation software package Quokka, using an input value for the emitter contact recombination of  $1210 \text{ fA}/\text{cm}^2$ , which corresponds to the fitted value  $J_{0,c}$  from experimentally measured  $V_{oc}$  values. For front illuminated samples, Quokka calculates  $V_{oc}$  values that lead to a fitted  $J_{0,c}$  of  $1386 \text{ fA}/\text{cm}^2$  for the emitter, while for rear illumination and the same input value, the fitted  $J_{0,c}$  value becomes much higher,  $1910 \text{ fA}/\text{cm}^2$ . This is shown in Table II.

**Table II:** Fit of  $J_{0,c}$  values in  $\text{fA}/\text{cm}^2$ , from  $V_{oc}$  measurements and from  $V_{oc}$  values resulting from test structure simulations in Quokka, obtained with different sample orientations. The Quokka input value for  $J_{0,c}$  was  $1210 \text{ fA}/\text{cm}^2$

Orientation	Measurement	Simulation
Front illumination	1217	1386
Rear illumination	1834	1901

The fits from the simulated and measured  $V_{oc}$  values show the same trend for front and rear illuminated conditions. However, both situations appear not to lead to

the right value. Even for front illuminated samples, which is the condition closest to the IBC cell measurement, a small correction of the fitted  $J_{0,c}$  value will be necessary. At the moment, we are investigating and validating this further.

## 6 CONCLUSION

We showed that the firing temperature, metallization paste and emitter profile cause a significant change in  $J_{0,c}$  and  $R_{contact}$  of the emitter contact.

Based on the fitted  $J_{0,c}$  and  $R_{contact}$  values for the different emitter cases, and the introduction of a lighter FFE, we foresee that we can improve the performance of the Mercury IBC cell to at least 21.5% with only small process modifications like different emitter and FFE profiles and contacting paste.

Although more validation is needed to obtain the correct absolute numbers for  $J_{0,c}$ , we can roughly estimate from the raw  $V_{oc}$  data what the gain could be in case of a process change.

## 7 ACKNOWLEDGEMENTS

This work was supported by the Dutch Ministry of Economic Affairs, within the TKI framework, project IBCense.

## REFERENCES

- [1] I. Cesar, N. Guillevin, A.R. Burgers, A.A. Mewe, M. Koppes, J. Anker, L.J. Geerligs, and A.W. Weeber, "Mercury: a back junction back contact front floating emitter cell with novel design for high efficiency and simplified processing" *Energy Procedia*, vol 55 2014, p. 633.
- [2] P. Spinelli, P. Danzl, N. Guillevin, A. Mewe, S. Sawallich, A. Vlooswijk, B. van de Loo, E. Kessels, M. Nagel, and I. Cesar, "High-resolution sheet resistance mapping to unveil edge effects in industrial IBC solar cells", *SiliconPV*, 2016, Chambéry, to be published.
- [3] A. Fell, "A free and fast 3D/2D solar cell simulator featuring conductive boundary and quasi-neutrality approximations," *IEEE Transactions on Electron Devices*, Vol 60 (2), pp. 733–738, 2012.
- [4] T. Fellmeth, A. Born, A. Kimmerle, F. Clement, D. Biro, and R. Preu, "Recombination at Metal-Emitter Interfaces of Front Contact Technologies for Highly Efficient Silicon Solar Cells," *Energy Procedia* vol 8, 2011, p. 115
- [5] E. Kossen, "Contacting high ohmic boron emitters with a screen print paste on n-Pasha", *Metallization Workshop*, 2016, Constance